Li Proton Storage Ring

Runze Li

June 25 2020

1 Lattice Design

From May 20 to June 13, in this project a proton storage ring was designed using MADX. This ring stores 2.5MeV proton beam in a 40 meters decagon-like structure, as shown in figure 1.

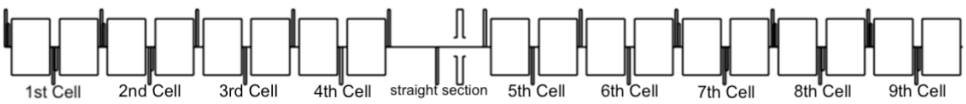

Figure 1: Structure of Li Ring

As shown in this figure, the ring structure is consisted by 10 parts: one straight section and nine focusing defocusing (fodo) cells. The fodo cells are divided into two groups, where the 3rd, 4th, 5th, and 6th cells are disperssion suppressors (DS), and the rest are normal fodo cells. The structure of a single normal fodo cell is shown in figure 2:

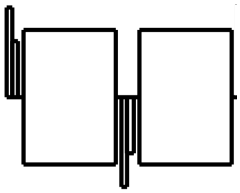

Figure 2: Structure of Normal FODO Cell

The normal FODO cell on the is a 4 meters sequence with quadrupole magnets, sextupole magnets, and sector bending dipoles. Each of the sector

bending dipole deflects the proton with kinetic energy 2.5MeV by $\frac{2\pi}{14}$, and the strength of quadrupoles are matched in MADX to make the horizontal phase advance $\frac{\pi}{4}$. The two sextupoles in each of the normal fodo cells correct the chromaticity effect by making DQ1 and DQ2 both 1 for one turn in this ring. All 5 normal fodo cells in this ring are the same, and the detail is shown in the following table:

Table 1: elements in normal fodo cells

element	length (m)	characteristic
dipole	1.6	bending angle = $\frac{2\pi}{14}$
quadrupole	0.1	k = $\pm$5.534
1st sextupole	0.1	k2 = 6.30213
2nd sextupole	0.1	k2 = -7.17147

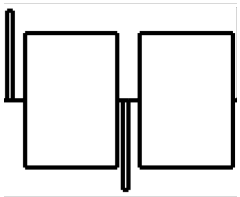

Figure 3: Structure of Dispersion Suppressor Cell

The dispersion suppressor shown in Figure 3 is a 4 meters sequence of quadrupoles and sector bending dipoles and is used to make dispersion 0 in the straight section. Each of the bending dipole deflects the proton beam by $\frac{2\pi}{28}$ (i.e. half of the deflection angle in the normal fodo cell), and the strength of quadrupole is matched to make dispersion 0 in the whole straight section. Since this constrain requires both dispersion and its derivative to be 0 at the beginning of straight section, it is actually two constrains which requires two variables in matching. As a result, the 3rd cell and 4th cell, although both are dispersion suppressor cells, have different quadrupole strength. The detail of dispersion suppressor cell is shown in the following table:

Table 2: elements in 3rd and 6th DS cells

element	length (m)	characteristic
dipole	1.6	bending angle = $\frac{2\pi}{28}$
quadrupole	0.1	k = $\pm$5.4828

Table 3: elements in 4rd and 5th DS cells

element	length (m)	characteristic
dipole	1.6	bending angle = $\frac{2\pi}{28}$
quadrupole	0.1	k = $\pm$5.54988

In the straight section there is no bending dipole, and the strength of quadrupoles are k = $\pm$5.55 set to make beta function periodic. Also, the quadrupole strength here is used to adjust phase advance. It is set to avoid horizontal and vertical phase advance to be integer or half integer since such phase advance value makes the system unstable under magnetic imperfection, and in the next part it will be changed to get tunes that induce resonance.

As a result, the ring (without rf cavity so far) has dispersion function shown in figure 4. In the straight section from 16m - 20m on the horizontal axis, the dispersion is suppressed to 0.

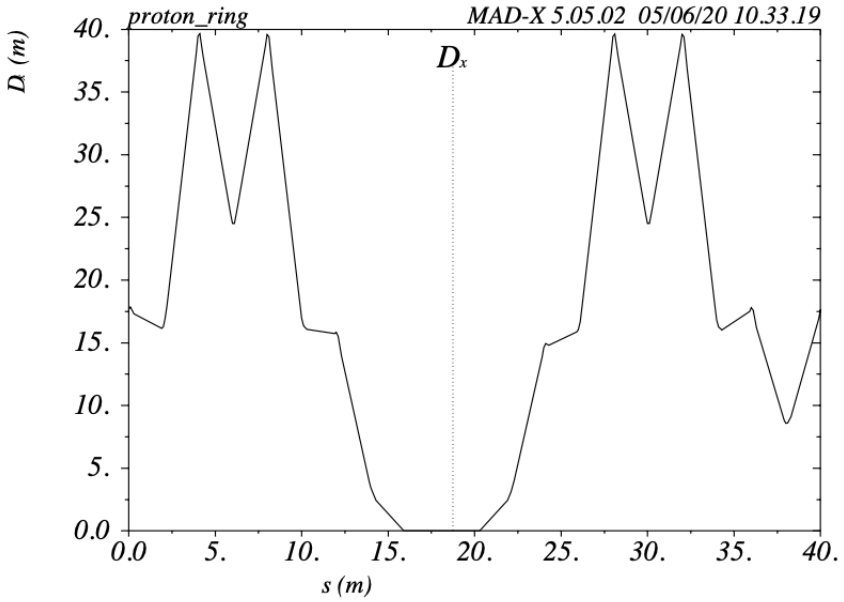

Figure 4: Dispersion along the Ring

Then a rf cavity is put in the 0 dispersion region to create stable bunched beam. Since the target beam and length of Li ring is similar to that of Integral Optic Test Accelerator (IOTA) in Fermilab, the rf cavity design mimic its

parameters and goals as well. As a proton storage ring, ϕ_s, the phase of synchronous particle, is set to be 0. The harmonic humber h is set to be 4, which is the same as IOTA ring. The voltage used in the rf cavity is set to make the rms momentum deviation of proton 0.1%, i.e. $\delta_{rms} = \frac{\delta p}{p_o} = \frac{1}{1000}$. The relation of δ_{rms} with other lattice parameters is:

$$\delta_{rms} \propto (\frac{\omega_0}{\pi\beta^2 E})^{\frac{1}{2}} (\frac{heV|cos(\phi_s)|}{2\pi\beta^2 E|\eta|})^{\frac{1}{4}}$$

The synchronous frequency ω_0, beam energy E, harmonic number h, and phase of synchronous particle ϕ_s are the same for Li ring and IOTA, and in IOTA , the voltage is set to be 400Volt to make $\delta_{rms} = \frac{1}{1000}$, the voltage that Li ring needs can be calculated by:

$$\frac{V}{|\eta|} = \frac{V'}{|\eta'|}$$

with phase slip factor $\eta = \alpha_p - \frac{1}{\gamma^2}$. The value of momentum compaction factor α_p can be obtained from twiss output of lattice design and γ is the Lorentz factor. As the result, the voltage of Li ring is set to be 327Volt.

2 Particle Tracking

After the lattice sequence was determined, particle tracking is performed in MADX to get the poincare map in order to visualize the effect of nonlinear resonance. The rms emittance of particle distribution is determined to be 1μm, and initial twiss parameters γ_0 and β_0 can be obtained from twiss output. Then, according to the relation $x_{rms} = \sqrt{\epsilon_{rms}\beta}$ and $x'_{rms} = \sqrt{\epsilon_{rms}\gamma}$, the rms value in phase space can be calculated as a vector in 4D phase space:

$$\vec{p_{rms}} = \begin{bmatrix} x_{rms} \\ x'_{rms} \\ y_{rms} \\ y'_{rms} \end{bmatrix} \tag{1}$$

In this simulation 8 particles with initial position $\vec{p_1} = \vec{p_{rms}}$, $\vec{p_2} = 5\vec{p_{rms}}$, ..., $\vec{p_8} = 40\vec{p_{rms}}$ are prepared and tracked for 5000 turns. The poincare map is plotted in both resonance and non resonance case by adjusting strength of quadrupoles in the straight section to reach tunes that induce resonance. In order to show the nonlinear effect of sextupoles, each tracking is performed with and without sextupoles. The following figures show the tracking results.

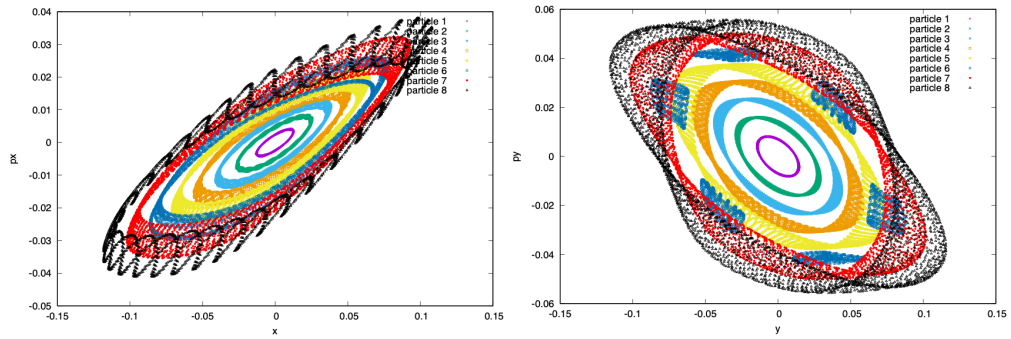

Figure 5: x-x' and y-y' phase space map in non-resonance case

Figure 5 shows the poincare map for x-x' and y-y' plane. In this case the quadrupoles in the straight section has K = 5.55 which corresponds to tune $\nu_x = 2.2389$ and $\nu_y = 1.8278$. Since the resonance driven by sextupoles requires $|a|\nu_x + |b|\nu_y = m$ and $|a| + |b| = 3$ for integer a, b, m, this ν_x and ν_y value does not correspond to any resonance condition (actually 2.24 + 2*1.829 = 5.898 so it is still close to 6). In this plot we can see that for particles close to the center, i.e. those $\vec{p_n} = n\vec{p_{rms}}$ with smaller n, the plot is closer to an ellipse because the perturbation of sextupoles is smaller. In this case the Hill's equation is not perturbed too much so a particle has a fixed emittance in any given place of the ring. For particles that start further away from center, the nonlinear effect becomes stronger so we see the ellipse get shifted comparing to figure 6 which shows this setup without any sextupoles. As shown in Figure 6, every particle, no matter where it starts on the phase space map, forms an ellipse.

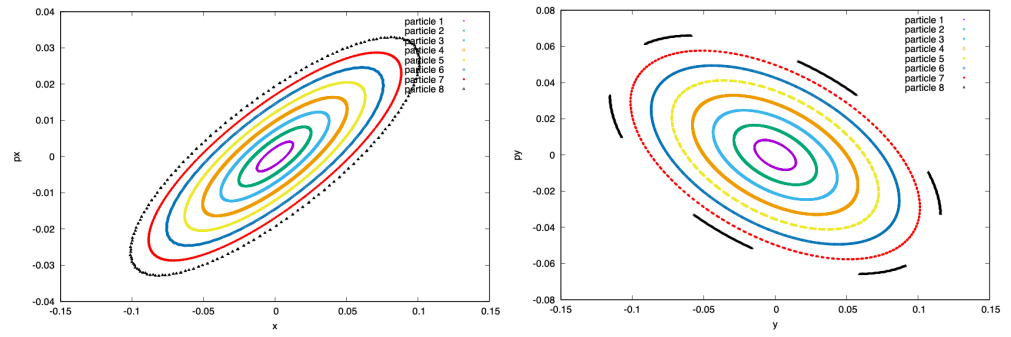

Figure 6: x-x' and y-y' phase space map without nonlinear effect

One fact about these plots is that the ellipse on x-x' and y-y' phase space tilts to different directions. This fact can be explained by the analytical solution of Hill's equation. For Hill's equation $x'' + K(s)x = 0$, the solution with twiss parameters is:

$$x = \sqrt{2\beta J} cos\phi$$
$$x' = -\sqrt{\frac{2J}{\beta}}(sin\phi + \alpha cos\phi)$$

with $\alpha = -\frac{\beta'}{2}$. Since the focusing quadrupole on horizontal direction is a defocusing quadrupole on vertical direction and vice versa, the sign of α on horizontal and vertical plane is opposite, which makes the ellipse on x-x' and y=y' tilt in different directions.

Then the strength of quadrupole is changed to K = 7.51. In this case the tune on x axis is $\nu_x = 2.323 \approx \frac{7}{3}$, which causes the resonance of sextupole. Figure 7 shows the tracking result in this case on x-x' phase space.

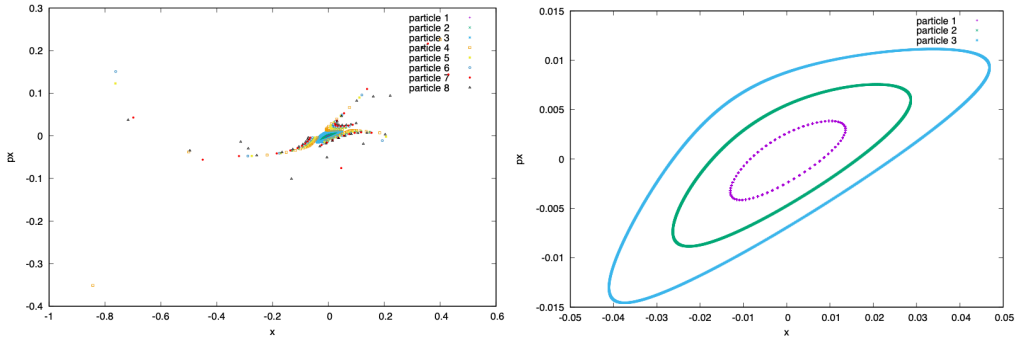

Figure 7: x-x' phase space with resonance $3\nu_x = m$

The left plot shows the tracking result of all 8 particles, and only 3 of them closest to the center survived without lost. This plot clearly shows the characteristic separatrix at 3rd order resonance with $3\nu_x = m$, which has perturbed ellipse emittance bounded by a separatrix defined by 3 unstable fixed points. The right plot shows the phase space emittance of those 3 particles that did not get lost in 5000 turns. The fact that close to the center when the sextupole perturbation is small the emittance is still elliptical can still be observed. Comparing to the plot in Figure 8 which shows the x-x' phase space emittance without sextupole, we can see the effect of non-linear resonance clearly.

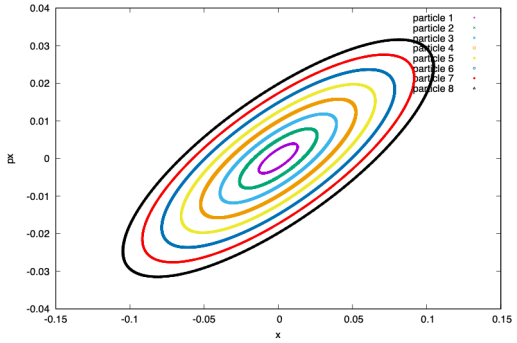

Figure 8: x-x' phase space without sextupole

Another case of nonlinear resonance is shown in Figure 9. In this case the strength of quadrupole in the straight section is set to K = 1 to make $\nu_x = 2.114$ and $\nu_y = 1.774$, so $2\nu_x + \nu_y = m$. As shown in this plot, particle 7 and 8 are lost after several turns, and the shape of emittance is elliptical in the center, and it perturbed when nonlinear effect is stronger.

However, since the textbook only has expected separatrix for $3\nu_x = m$ case, I am not sure if this plot is what we expect in $2\nu_x + \nu_y = m$ resonance.

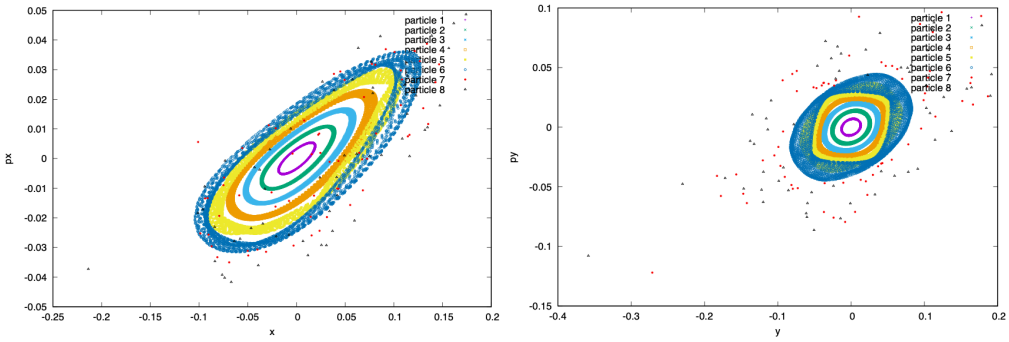

Figure 9: x-x' and y-y' phase space with resonance $2\nu_x + \nu_y = m$

3 Dynamic Aperture

In order to measure the Dynamic Aperture of Li Ring, 5000 particles are tracked for 10000 turns and those that survive in the end are recorded. These 5000 particles are initialized according to:

$$x = 1.5 * n * \sqrt{2\beta_x J} cos\phi$$
$$x' = 0$$
$$y = 1.5 * n * \sqrt{2\beta_y J} sin\phi$$
$$y' = 0$$
$$\phi \in [0, \frac{\pi}{2}]$$
$$n \in [1, 100].$$

There are 100 values of n and 50 values of ϕ. After tracking for 10000 turns, in x-y space all survivors and all initial particles are shown in the left plot of Figure 10. Then for each ϕ the largest initial x and y values for all survivors are extracted separately and made into a scatter plot on the right. These plot has both axis normalized by the rms radius, and it shows the maximum initial value of x and y that a particle can have while surviving through 10000 turns in Li Ring. One feature in the dynamic aperture plot is that for $\phi \approx \frac{\pi}{6}$, the aperture is much smaller than that of other angle. One possible reason is due to the large beta beating effect, as shown in the beta function of Li Ring in Appendix I.

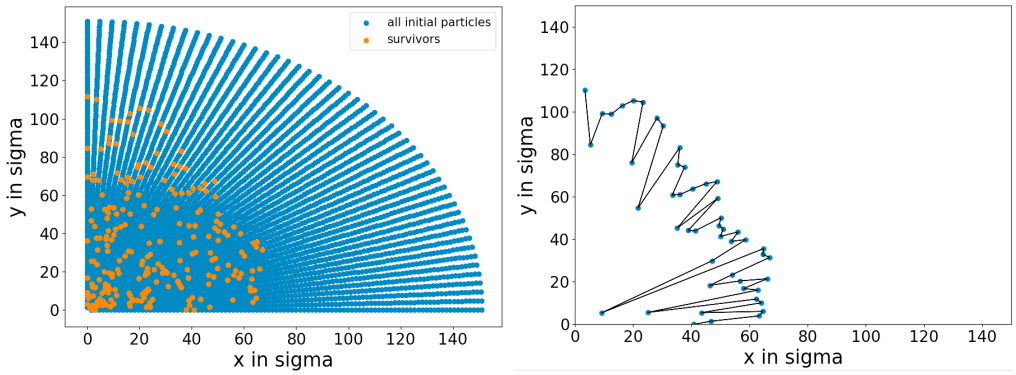

Figure 10: Survivors vs Initial Particles(left) and Dynamic Aperture(right)

4 Tune Footprint

The tune footprint of Li Ring is plotted in a similar way. 10000 muons are space in $x = 0.1n_x * \sqrt{2\beta_x J}$ and $y = 0.1n_y * \sqrt{2\beta_y J}$, with nx and ny both from 1 to 100. The initial momentum deviation $\frac{dp}{p}$ is set to 0. The dynap command in MADX tracks them for 1024 turns and get the $tune_x$

and $tune_y$ for all surviving particles. The x and y tune spread is shown in Figure 11. Since the value q1 and q2 calculated from twiss functions (as mentioned previously) are $\nu_x = 2.2389$ and $\nu_y = 1.8278$, and the tune value calculated by dynap is confined with in [0, 0.5], the expected tune after converting is $tune_x = 0.2389$ and $tune_y = 0.1722$, which is the center of tune spread in Figure 11. Although we set $\frac{dp}{p} = 0$ for all initial particles, since there exists the nonlinear effect of sextupole and the initial x and y position of these particles are different, some small extent of tune spread can still be observed.

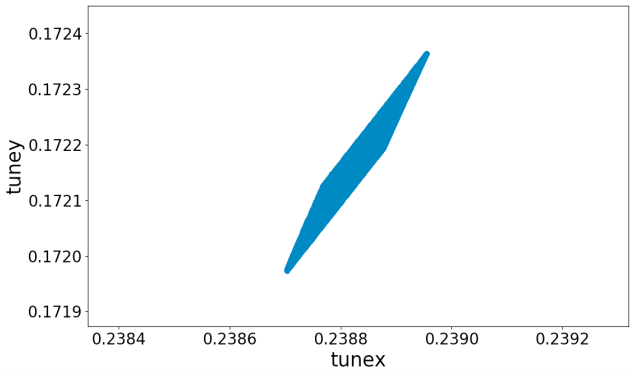

Figure 11: Tune Footprint

5 Appendix I

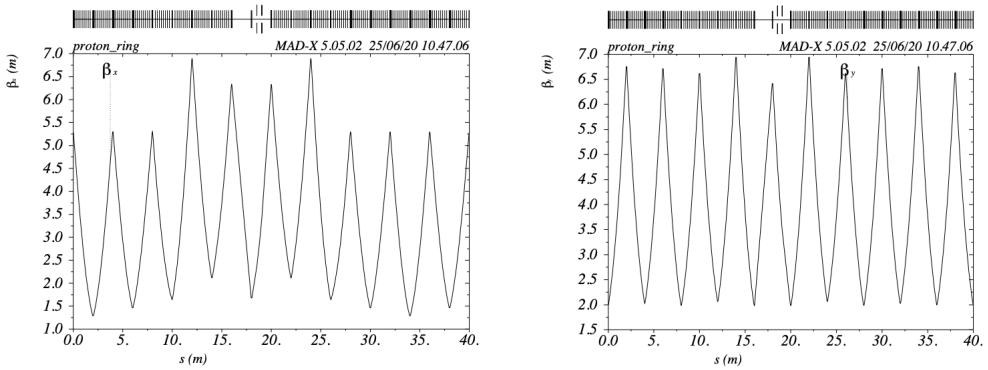

Figure 12: Beta Function for Li Ring(after makethin)

6 Appendix II

The same percedure is performed on IOTA Lattice. The result of tune footprint is shown in Figure 13. Similar with the tune footprint in Li Ring, here the $\frac{dp}{p}$ is set to 0, however, due to the strong nonlinear effect in iota, there is still the tune spread.

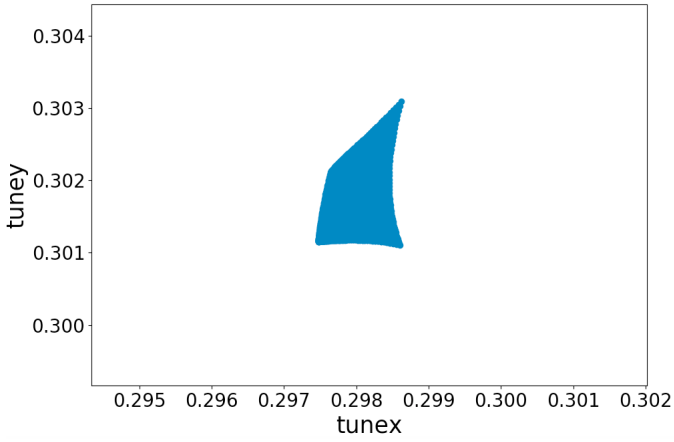

Figure 13: IOTA Tune Footprint

Figure 14 shows the dynamic aperture plot of iota ring. In this case the beam inside iota is assumed to be 150MeV electrons.

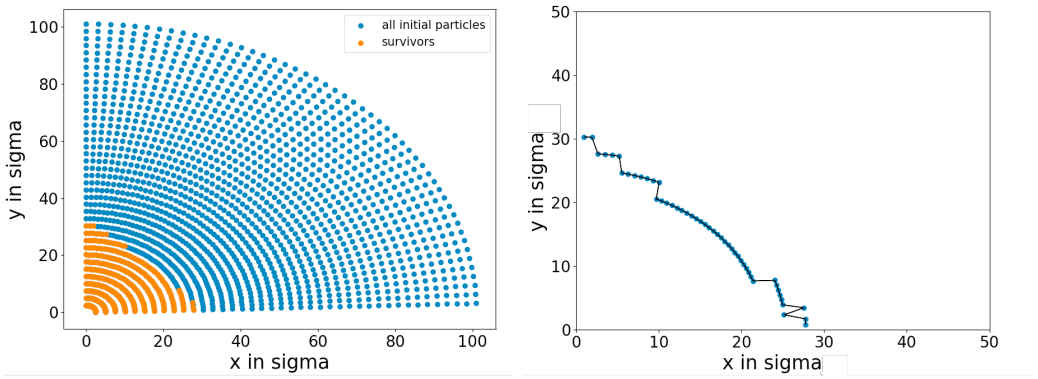

Figure 14: Survivors (left) and Dynamic Aperture(right) of IOTA